Chinese Chemical Letters 34 (2023) 107498

Contents lists available at ScienceDirect

Chinese Chemical Letters

journal homepage: www.elsevier.com/locate/cclet

Design and fabrication of highly hydrophilic magnetic material by anchoring L-cysteine onto chitosan for efficient enrichment of glycopeptides

Binfen Zhao[a], Wenhui Xu[a], Jiutong Ma[a], Qiong Jia[a,b,*]

[a] College of Chemistry, Jilin University, Changchun 130012, China
[b] Key Laboratory for Molecular Enzymology and Engineering of Ministry of Education, School of Life Sciences, Jilin University, Changchun 130012, China

ARTICLE INFO

Article history:
Received 18 January 2022
Revised 12 April 2022
Accepted 7 May 2022
Available online 11 May 2022

Keywords:
Chitosan
L-cysteine
Hydrophilic material
Glycopeptide
Enrichment

ABSTRACT

Hydrophilic interaction liquid chromatography (HILIC) has been recognized as an effective strategy for glycopeptide enrichment. Hydrophilic materials pave the way to solve the limit of low enrichment capacity and poor selectivity. The present study is the first attempt to combine chitosan (CS) and L-cysteine (L-Cys) to design a novel hydrophilic material focusing on glycopeptide enrichment. CS containing a large number of hydrophilic amino and hydroxyl groups has unique chemical properties, which makes it a very attractive biomaterial for glycopeptide enrichment. The excellent hydrophilicity of zwitterionic molecule L-Cys inspires the idea of anchoring L-Cys onto CS to design a novel hydrophilic material (named as Fe_3O_4@CS@Au-L-Cys) for the capture of low abundance glycopeptides. To be specific, Au nanoparticles (Au NPs) was introduced into CS-coated Fe_3O_4 *via* electrostatic interaction and served as bridges to anchor L-Cys onto the surface of CS through strong Au-S bond interaction. The prepared Fe_3O_4@CS@Au-L-Cys exhibited strong affinity, low detection limit (0.5 fmol/μL HRP), high selectivity (HRP/BSA with a molar ratio of 1:1000) for glycopeptides. Moreover, successful application of glycopeptide enrichment in human serum and saliva by Fe_3O_4@CS@Au-L-Cys was achieved. A satisfactory data set indicates that Fe_3O_4@CS@Au-L-Cys has promising potential in the application of glycopeptide enrichment in real complex bio-samples and for related glycoproteome research.

Protein glycosylation, as one of the most important and common post-translational modifications, is consanguineously relevant to multiple biological processes [1]. It is well known that glycoproteins serve as many disease markers and treatment labels in clinical diagnoses, but the low abundance and weak ionization efficiency of glycoproteins make the detection of glycoproteins challenging in mass spectrometry (MS) measurements [2,3]. Until now, a wide variety of strategies for enriching glycopeptides have been studied including lectin affinity chromatography [4,5], hydrazide chemistry [6,7], boronic acid affinity chromatography [8–11], and hydrophilic interaction liquid chromatography (HILIC) [12–16]. Among them, HILIC method for glycopeptide enrichment based on hydrophilic partitioning and other interactions such as hydrogen bonding, electrostatic and dipole interactions, receives increasing attention because of its high sensitivity, good reproducibility, excellent MS compatibility, and easy operation [17,18]. Accordingly, many kinds of hydrophilic materials have been designed and used for glycopeptide enrichment such as magnetic particles, graphene-based materials, and metal-organic frameworks [19–21]. Nevertheless, these materials still have difficulties in modifying high density of hydrophilic groups due to large steric hindrance, complicated synthesis steps, and harsh conditions [22,23].

Chitosan (CS), as a kind of natural polymer normally obtained by alkaline deacetylation of chitin, has become a very attractive biomaterial with non-toxicity, biocompatibility, as well as biodegradability [24,25]. In addition, high density of amino and hydroxyl groups in CS molecule endow it with hydrophilicity and abundant reactive sites. CS has been used to design adsorbents toward a lot of substances, such as metal ions [26,27], dyes [28,29], environmental pollutants [30,31], and proteins [32,33]. Based on the hydrophilic interactions between plenty of hydrophilic groups of CS and glycopeptides, CS-coated magnetic colloidal nanocrystal cluster [34], highly cross-linked porous CS microsphere [35], and honeycomb CS membrane [23] were synthesized and used for glycopeptide enrichment. Unfortunately, it should be noted that the inherent inflexibility and poor acid resistance of CS are not conducive to the enrichment performance [36,37]. As an alternative,

* Corresponding author.
E-mail address: jiaqiong@jlu.edu.cn (Q. Jia).

https://doi.org/10.1016/j.cclet.2022.05.012
1001-8417/

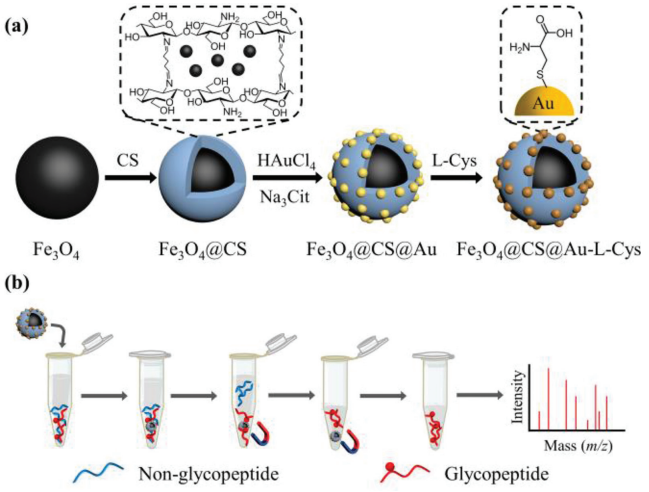

Scheme 1. (a) Synthesis process of Fe_3O_4@CS@Au-L-Cys and (b) typical enrichment process of glycopeptides by Fe_3O_4@CS@Au-L-Cys.

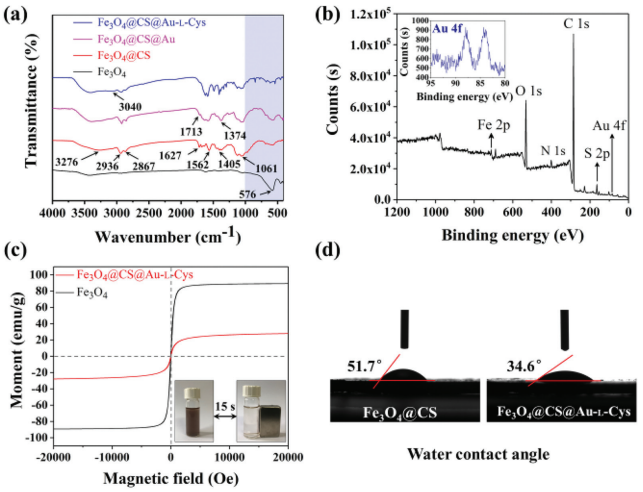

Fig. 1. (a) FT-IR spectra of Fe_3O_4, Fe_3O_4@CS, Fe_3O_4@CS@Au, and Fe_3O_4@CS@Au-L-Cys. (b) XPS pattern of Fe_3O_4@CS@Au-L-Cys. (c) VSM profiles of Fe_3O_4 and Fe_3O_4@CS@Au-L-Cys. (d) Water contact angles of Fe_3O_4@CS and Fe_3O_4@CS@Au-L-Cys.

the introduction of functional groups onto CS makes it possible to obtain improved enrichment capacity. For instance, poly(glycerol methacrylate) and iminodiacetic acid with hydrophilic groups were grafted onto the surface of CS to increase the hydrophilicity, thus enhancing the enrichment performance toward glycopeptides [38]. It can be deduced that the introduction of hydrophilic functional groups onto the surface of CS plays a positive role in improving the affinity between glycopeptides and CS-based HILIC materials, while the search of hydrophilic molecule that can be grafted onto CS is still on its way.

Zwitterionic molecules containing both positive and negative groups exhibit attractive hydrophilicity [39]. L-Cysteine (L-Cys), as a zwitterionic hydrophilic compound, possesses polar groups including thiol, amino, and carboxyl groups, so L-Cys has shown great potential in the construction of hydrophilic materials for the efficient enrichment of glycopeptides [22,40-42]. Besides, the affinity between thiol groups of L-Cys and metal nanoparticles allows L-Cys to be easily anchored to various types of substrates. Wu *et al.* [43] prepared L-Cys-modified silica microsphere columns for glycopeptide enrichment. In Ma *et al.*'s study [44], L-Cys-functionalized metal-organic framework with high hydrophilicity was applied to the capture of glycopeptides. There is no doubt that higher hydrophilicity will be obtained if L-Cys is anchored to a hydrophilic substrate. Motivated by the above information, a HILIC material designed by anchoring L-Cys onto the surface of hydrophilic CS can be anticipated to capture glycopeptides efficiently. To the best of our knowledge, no HILIC material combining the hydrophilicity of CS and L-Cys has been applied for glycopeptide enrichment.

Herein, we developed magnetic L-Cys-functionalized CS (designed as Fe_3O_4@CS@Au-L-Cys) and applied to the specific capture of glycopeptides by utilizing the hydrophilicity of CS and L-Cys. The preparation of Fe_3O_4@CS@Au-L-Cys nanocomposites is illustrated in Scheme 1. CS was crosslinked with glutaraldehyde as the crosslinker and then coated onto the surface of Fe_3O_4 to obtain Fe_3O_4@CS. Au nanoparticles (Au NPs) were embedded onto the surface of Fe_3O_4@CS by electrostatic interaction to obtain Fe_3O_4@CS@Au, and then L-Cys molecules were grafted onto Fe_3O_4@CS@Au *via* Au-S bond between Au NPs and –SH of L-Cys to obtain Fe_3O_4@CS@Au-L-Cys. The synthesized Fe_3O_4@CS@Au-L-Cys possesses the following advantages. Firstly, abundant hydrophilic groups of CS provide not only attachment sites for Au NPs but also affinity sites toward glycopeptides. Secondly, the introduction of L-Cys with hydrophilic groups enhances hydrophilicity of this material, in other words, the hydrophilicity of both CS and L-Cys contributes to the efficient enrichment of glycopeptides. Thirdly, this material with superparamagnetism can be rapidly separated by an external magnet, which facilitates further MS analysis. Fe_3O_4@CS@Au-L-Cys nanocomposites exhibit high enrichment efficiency and selectivity for glycopeptide enrichment and were successfully applied to the enrichment of glycocpeptides from standard proteins digests and real complex bio-samples.

To confirm the successful synthesis of Fe_3O_4@CS@Au-L-Cys, FT-IR spectra of Fe_3O_4, Fe_3O_4@CS, and Fe_3O_4@CS@Au-L-Cys were determined. As indicated in Fig. 1a, the stretching vibration of Fe–O at 576 cm^{-1} exists in the spectrum of unmodified Fe_3O_4. It can be seen that the peaks at 1061 cm^{-1} (C–O–C stretching vibration in CS ring backbone), 1405 cm^{-1} (–C–O stretching of primary alcoholic group in CS), 1627 cm^{-1} (C=N stretching vibration formed by the reaction of CS and glutaraldehyde), and 2936 and 2867 cm^{-1} (asymmetric and symmetric stretching vibration of C–H bond) exist in the spectrum of Fe_3O_4@CS. In addition, the peak at 1562 cm^{-1} can be attributed to N–H bending vibration and the broad absorption band at around 3276 cm^{-1} represents O–H stretching vibration [45,46]. All the above evidences confirm that CS was successfully coated onto Fe_3O_4 surface, and both amino and hydroxyl groups are present on the surface of Fe_3O_4@CS. Au NPs formed by Na_3Cit as the reducing agent were embedded onto the surface of Fe_3O_4@CS, so the spectrum of Fe_3O_4@CS@Au shows peaks at 1713 and 1374 cm^{-1} belonging to C=O and C–O stretching vibrations of carboxyl groups. In the spectrum of Fe_3O_4@CS@Au-L-Cys, the appearance of wide shape characteristic peak of –COOH at 3040 cm^{-1} and the fingerprint peaks of L-Cys below 1000 cm^{-1} (shaded area) clearly confirm L-Cys functionalization [44].

The elemental composition of Fe_3O_4@CS@Au-L-Cys was tested by XPS determination. As shown in Fig. 1b, in addition to the characteristic peaks of Fe 2p, C 1s, N 1s, and O 1s, the signals of S 2p and Au 4f also appear, indicating the introduction of Au NPs and the grafting of L-Cys. Additionally, TEM images of Fe_3O_4@CS and Fe_3O_4@CS@Au-L-Cys (Fig. S1 in Supporting information) demonstrate the coating of CS onto Fe_3O_4 and the introduction of Au NPs with an average diameter of 40 nm. In summary, the above FT-IR, XPS, and TEM results clearly indicate the successful preparation of Fe_3O_4@CS@Au-L-Cys.

XRD patterns of Fe_3O_4, Fe_3O_4@CS, Fe_3O_4@CS@Au, and Fe_3O_4@CS@Au-L-Cys were determined from 20° to 80° (2θ).

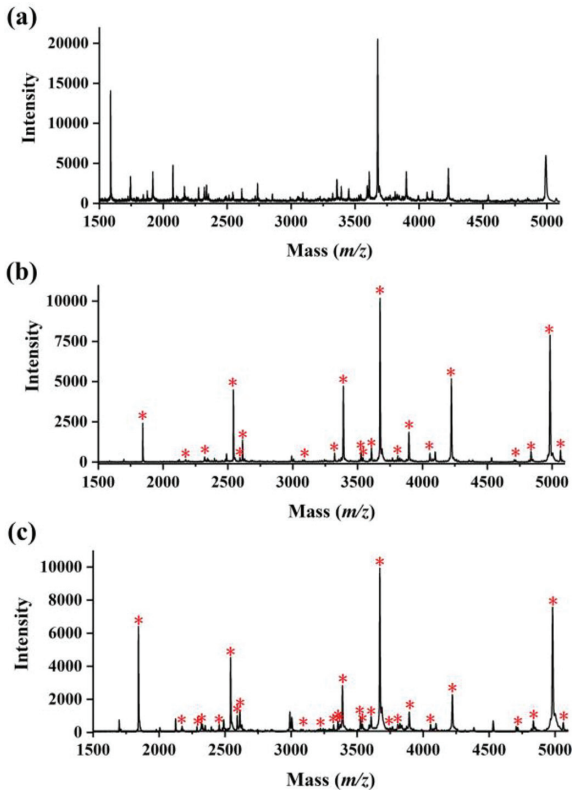

Fig. 2. MALDI-TOF mass spectra of tryptic digests of 1000 fmol/μL standard HRP (a) before enrichment and after enrichment by (b) Fe_3O_4@CS and (c) Fe_3O_4@CS@Au-L-Cys. "*" indicates glycopeptide.

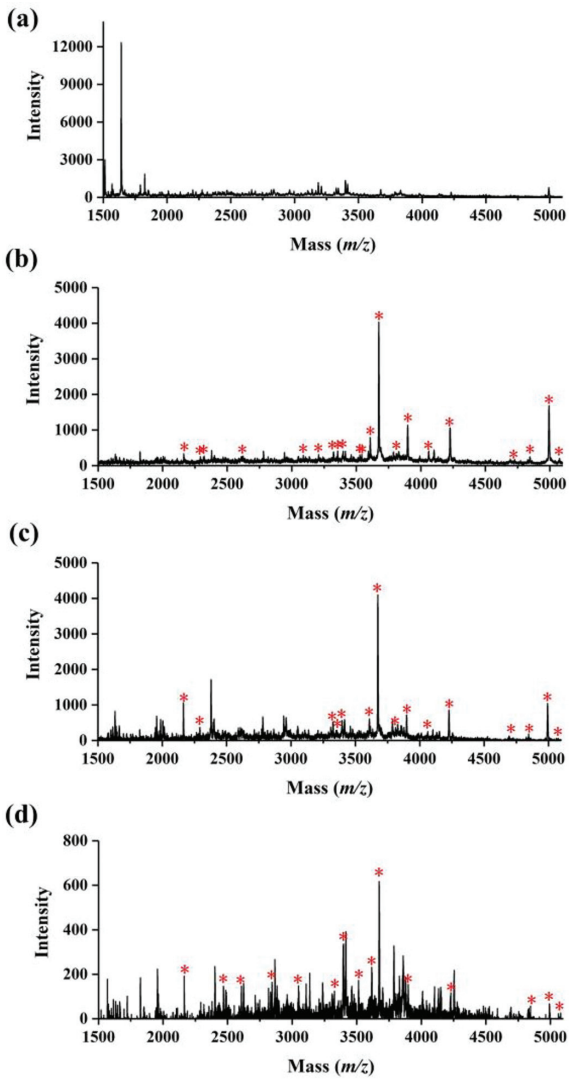

Fig. 3. MALDI-TOF mass spectra of mixtures of HRP and BSA tryptic digests with a molar ratio of (a) 1:100 without enrichment and (b) 1:100, (c) 1:500, and (d) 1:1000 enriched by Fe_3O_4@CS@Au-L-Cys. "*" indicates glycopeptide.

As shown in Fig. S2a (Supporting information), six diffraction peaks at 2θ of 30.2°, 35.6°, 43.2°, 53.5°, 57.1°, and 63.0° exist in the curve of Fe_3O_4 NPs, which are consistent with those of standard Fe_3O_4 according to JCPDS No. 19–0629 [47,48]. There are no other diffraction peaks in the spectrum of Fe_3O_4@CS, indicating that the coating of CS does not damage the crystal structure of Fe_3O_4. In the case of Fe_3O_4@CS@Au, there are not only the characteristic peaks of Fe_3O_4, but also four additional peaks of Au NPs at 2θ of 38.3°, 44.6°, 64.8°, and 77.7°, which can be attributed to (111), (200), (220), and (311) planes of Au NPs (JCPDS No. 04–0784) [17]. Such results prove that Au NPs were successfully loaded onto Fe_3O_4@CS. While for Fe_3O_4@CS@Au-L-Cys, the characteristic peaks of Fe_3O_4 and Au NPs also appear, indicating that the introduction of L-Cys does not affect the crystal structure of Fe_3O_4 and Au.

The thermal stability of Fe_3O_4 and Fe_3O_4@CS@Au-L-Cys nanocomposites was characterized within the temperature range from 30 °C to 800 °C. As shown in Fig. S2b (Supporting information), Fe_3O_4 NPs show excellent thermal stability and the weight loss is only 2.2%. However, the thermal stability of Fe_3O_4@CS@Au-L-Cys nanocomposites is not as good as that of Fe_3O_4 NPs. In the thermogram of Fe_3O_4@CS@Au-L-Cys nanocomposites, the sight weight loss (~10%) below 150 °C can be ascribed to the removal of water in the material. In the range from 150 °C to 460 °C, there is an obvious wide range of weight loss (~47.15%), which might be caused by the rapid decomposition of CS and L-Cys. With further increase of temperature (>460 °C), the material exhibits slow weight loss (~11.16%), which can be attributed to the further degradation of the substance generated by CS degradation [49].

The magnetic property of Fe_3O_4@CS@Au-L-Cys was investigated by using the magnetic hysteresis loop analysis. As shown in Fig. 1c, the maximum saturation magnetization value of Fe_3O_4@CS@Au-L-Cys is 27.9 emu/g. Compared to Fe_3O_4, the decrease in saturation susceptibility of Fe_3O_4@CS@Au-L-Cys is due to the introduction of the non-magnetic shell including CS and L-Cys. Nevertheless, Fe_3O_4@CS@Au-L-Cys can gather within 15 s using an external magnet, indicating that the material has superparamagnetic characteristics to guarantee its rapid magnetic separation from solution. Additionally, the stability of Fe_3O_4@CS@Au-L-Cys was evaluated (Fig. S3 in Supporting information). Before and after storage for one month, the solutions are both clear with the help of a magnet, indicating that Fe_3O_4@CS@Au-L-Cys is stable.

To evaluate the hydrophilicity of Fe_3O_4@CS and Fe_3O_4@CS@Au-L-Cys, their water contact angel measurements were performed. As shown in Fig. 1d, the water contact angles of Fe_3O_4@CS and Fe_3O_4@CS@Au-L-Cys are 51.7° and 34.6°, demonstrating that both of them are typical hydrophilic materials. Obviously, the hydrophilicity of Fe_3O_4@CS@Au-L-Cys is higher than that of Fe_3O_4@CS, which further proves that the introduction of L-Cys contributes to the improvement of hydrophilicity. Fe_3O_4@CS@Au-L-Cys combining the hydrophilicity of CS and L-Cys has wide application prospects in the enrichment of hydrophilic glycopeptides.

The enrichment performance of Fe_3O_4@CS and Fe_3O_4@CS@Au-L-Cys toward glycopeptides from HRP tryptic digests (1000 fmol/μL) was investigated (Fig. 2). As displayed in Fig. 2a, the signal

intensity of glycopeptides was severely suppressed by MALDI-TOF MS direct analysis because of the presence of non-glycopeptides. However, after enrichment by Fe_3O_4@CS, the signals of glycopeptides were enhanced significantly and most of the interferences of non-glycopeptides were eliminated (Fig. 2b). This result implies that CS coated onto the surface of Fe_3O_4 NPs plays an essential role in the enrichment of glycopeptides owing to the hydrophilic groups in CS. Then, the enrichment of HRP tryptic digests with Fe_3O_4@CS@Au-L-Cys was performed and a total of 27 glycopeptides were identified in the MS spectrum (Fig. 2c). Detailed information of the enriched glycopeptides is listed in Table S1 (Supporting information). Obviously, based on the superior hydrophilicity of CS and L-Cys, more glycopeptides were identified with strong signals. As is expected, the introduction of hydrophilic L-Cys enhances the surface hydrophilicity and further promotes the affinity interaction with glycopeptides. Additionally, the enrichment of IgG tryptic digests by Fe_3O_4@CS@Au-L-Cys was evaluated (Fig. S4 in Supporting information). After enrichment by Fe_3O_4@CS@Au-L-Cys, 33 glycopeptides were clearly observed in the MS spectrum, indicating the unbiased enrichment ability of Fe_3O_4@CS@Au-L-Cys toward glycopeptides with different glycan types. Detail information of the enriched glycopeptides from IgG digests is listed in Table S2 (Supporting information).

Considering the low abundance of glycopeptides and the interference of non-glycopeptides in real bio-samples, it is crucial to evaluate the detection sensitivity and selectivity of glycopeptides. The sensitivity of glycopeptides with the developed Fe_3O_4@CS@Au-L-Cys MS method was studied by the enrichment of different concentration of HRP tryptic digests (100, 10, 1 and 0.5 fmol/μL). When the limit of detection is as low as 0.5 fmol/μL, 11 glycopeptides were selectively captured according to S/N ratio greater than 3 (Fig. S5 in Supporting information), which further indicates that Fe_3O_4@CS@Au-L-Cys has a good enrichment performance toward glycopeptides even at low concentrations.

The selectivity of glycopeptide enrichment by Fe_3O_4@CS@ Au-L-Cys was explored by adding BSA tryptic digests into HRP tryptic digests with different molar ratios. Few glycopeptides were detected without enrichment at HRP:BSA molar ratio is 1:100 (Fig. 3). After treated with Fe_3O_4@CS@Au-L-Cys, non-glycopeptides were effectively eliminated, while glycopeptides were clearly observed. It is noteworthy that glycopeptides can still be detected after enrichment with Fe_3O_4@CS@Au-L-Cys even when the molar ratio of HRP to BSA reaches 1:1000. The above results indicate that Fe_3O_4@CS@Au-L-Cys possesses great selectivity toward glycopeptides and can be expected to be applied as a highly efficient HILIC material for the capture of glycopeptides from real complex bio-samples.

For comparison, the detection sensitivity and selectivity of glycopeptides with Fe_3O_4@CS were also investigated (Figs. S6 and S7 in Supporting information). Obviously, the enrichment performance of Fe_3O_4@CS is inferior to that of Fe_3O_4@CS@Au-L-Cys for glycopeptides, proving that the introduction of hydrophilic L-Cys improves the glycopeptide enrichment performance. Besides, the comparison of the enrichment performance toward glycopeptides of Fe_3O_4@CS@Au-L-Cys with other HILIC materials is presented in Table S3 (Supporting information), which confirms the superior enrichment efficiency of Fe_3O_4@CS@Au-L-Cys.

Considering the practical application, the reusability of Fe_3O_4@CS@Au-L-Cys was evaluated by the enrichment of glycopeptides in HRP tryptic digests in consecutive times. The same preliminary optimized loading ($ACN/H_2O/TFA = 90/5/5$) and elution ($ACN/H_2O/TFA = 90/5/5$) buffers were used during the whole enrichment and elution procedures. Results are shown in Fig. S8 (Supporting information), demonstrating that there is no significant difference between the signals of glycopeptides after the first and fifth cycle, confirming the excellent repeatability and stability of Fe_3O_4@CS@Au-L-Cys toward glycopeptide enrichment. In a word, the developed HILIC strategy possesses satisfactory sensitivity, selectivity, and repeatability, which makes it greatly potential to be applied to real complex bio-samples determinations.

Encouraged by the above-obtained experimental results in the standard samples, Fe_3O_4@CS@Au-L-Cys was employed to enrich low-abundance glycopeptides from real complex bio-samples. Human serum, a commonly available clinical sample, was selected to evaluate the enrichment capacity of Fe_3O_4@CS@Au-L-Cys for glycopeptides. As shown in Figs. S9a and b (Supporting information), non-glycopeptides peaks dominate MS spectrum without enrichment, while 63 glycopeptides were identified from 2 μL normal human serum sample after Fe_3O_4@CS@Au-L-Cys enrichment. The detailed information is listed in Table S4 (Supporting information). To further evaluate the applicability of hydrophilic Fe_3O_4@CS@Au-L-Cys in complex bio-samples, human saliva was selected as another real complex bio-sample. Because the abundance of glycopeptides in human saliva is low, almost no corresponding glycopeptide peaks were found in the MS spectrum (Fig. S9c in Supporting information). Surprisingly, 37 glycopeptides were detected from 2 μL normal human saliva sample after enrichment with Fe_3O_4@CS@Au-L-Cys (Fig. S9d in Supporting information). Detailed information is listed in Table S5 (Supporting information). The comparison of the number of glycopeptides captured from real complex bio-samples of Fe_3O_4@CS@Au-L-Cys with the reported materials is shown in Table S6 (Supporting information). All the above results confirm that Fe_3O_4@CS@Au-L-Cys possessing high enrichment capacity toward glycopeptides has great application prospects in the analysis of real complex bio-samples.

In summary, the main feature of this work is the development of a novel hydrophilic material named as Fe_3O_4@CS@Au-L-Cys for the efficient enrichment of glycopeptides. Uniting good hydrophilicity and biocompatibility of CS and L-Cys and superparamagnetism of Fe_3O_4, Fe_3O_4@CS@Au-L-Cys exhibited good enrichment performance toward glycopetides from tryptic digests of standard glycoproteins. The glorious enrichment performance of this hydrophilic material was largely determined by the great hydrophilicity of L-Cys immobilized onto hydrophilic magnetic CS substrate. Moreover, in practical application, Fe_3O_4@CS@Au-L-Cys exhibited great availability in capturing glycopeptides from real bio-samples like human serum and saliva. We expect that this material can provide inspiration for the development of hydrophilic materials and be extended to capture potential biomarkers in clinical research.

Declaration of competing interest

The authors declare that they have no known competing financial interests or personal relationships that could have appeared to influence the work reported in this paper.

Acknowledgments

This work was financially supported by Open Project of State Key Laboratory of Supramolecular Structure and Materials, Jilin University, China (No. sklssm2022012) and the Fundamental Research Funds for the Central Universities, JLU, China.

Supplementary materials

Supplementary material associated with this article can be found, in the online version, at doi:10.1016/j.cclet.2022.05.012.

References

[1] H. Qi, L. Jiang, Q. Jia, Chin. Chem. Lett. 32 (2021) 2629–2636.
[2] X. Wang, Y. Liu, F. Li, Z. Li, Chin. Chem. Lett. 28 (2017) 1018–1026.
[3] H. Yang, F. Xu, K. Xiao, et al., Phenomics 1 (2021) 269–284.

[4] H. Zheng, T. Zhu, X. Li, et al., Anal. Chim. Acta 983 (2017) 141–148.
[5] D.F. Zielinska, F. Gnad, J.R. Wisniewski, M. Mann, Cell 141 (2010) 897–907.
[6] J. Chen, P. Shah, H. Zhang, Anal. Chem. 85 (2013) 10670–10674.
[7] Y. Zhang, M. Kuang, L. Zhang, et al., Anal. Chem. 85 (2013) 5535–5541.
[8] S. Kong, Q. Zhang, L. Yang, et al., Anal. Chem. 93 (2021) 6682–6691.
[9] H. Xiao, W. Chen, J.M. Smeekens, R. Wu, Nat. Commun. 9 (2018) 1692.
[10] Z. Xie, Y. Yan, K. Tang, C. Ding, Talanta 236 (2022) 122831.
[11] M.S. Sajid, F. Jabeen, D. Hussain, et al., J. Sep. Sci. 43 (2020) 1348–1355.
[12] T. Zhu, Q. Gu, Q. Liu, et al., Talanta 240 (2022) 123193.
[13] H. Zheng, X. Li, Q. Jia, ACS Appl. Mater. Interfaces 10 (2018) 19914–19921.
[14] C. Pu, H. Zhao, Y. Hong, et al., Anal. Chem. 92 (2020) 1940–1947.
[15] G. Qing, J. Yan, X. He, et al., TrAC Trends Anal. Chem. 124 (2020) 115570.
[16] B. Zhao, L. Jiang, Q. Jia, Chin. Chem. Lett. 33 (2022) 11–21.
[17] H. Qi, Z. Li, H. Zheng, et al., Chin. Chem. Lett. 30 (2019) 2181–2185.
[18] H.J. Zheng, J.T. Ma, W. Feng, Q. Jia, J. Chromatogr. A 1512 (2017) 88–97.
[19] J. Peng, Y. Hu, H. Zhang, et al., Anal. Chem. 91 (2019) 4852–4859.
[20] H. Zheng, J. Jia, Z. Li, Q. Jia, Anal. Chem. 92 (2020) 2680–2689.
[21] Y. Chen, Q. Sheng, Y. Hong, M. Lan, Anal. Chem. 91 (2019) 4047–4054.
[22] C. Xia, F. Jiao, F. Gao, et al., Anal. Chem. 90 (2018) 6651–6659.
[23] L. Zhang, S. Ma, Y. Chen, et al., Anal. Chem. 91 (2019) 2985–2993.
[24] P.S. Bakshi, D. Selvakumar, K. Kadirvelu, N.S. Kumar, Int. J. Biol. Macromol. 150 (2020) 1072–1083.
[25] Y. Li, X. Wang, Y. Wei, L. Tao, Chin. Chem. Lett. 28 (2017) 2053–2057.
[26] L. Zhang, Y. Zeng, Z. Cheng, J. Mol. Liq. 214 (2016) 175–191.
[27] Y. Zhu, Z. Bai, H. Wang, Chin. Chem. Lett. 28 (2017) 633–641.
[28] M. Vakili, M. Rafatullah, B. Salamatinia, et al., Carbohydr. Polym. 113 (2014) 115–130.
[29] J. Xing, X. Wang, J. Xun, et al., Carbohydr. Polym. 198 (2018) 69–75.
[30] I.O. Saheed, W.D. Oh, F.B.M. Suah, J. Hazard. Mater. 408 (2021) 124889.
[31] M. Keshvardoostchokami, M. Majidi, A. Zamani, B. Liu, Carbohydr. Polym. 273 (2021) 118625.
[32] U.J. Kim, Y.R. Lee, T.H. Kang, et al., Carbohydr. Polym. 163 (2017) 34–42.
[33] Z. Xiong, H. Qin, H. Wan, et al., Chem. Commun. 49 (2013) 9284–9286.
[34] C. Fang, Z. Xiong, H. Qin, et al., Anal. Chim. Acta 841 (2014) 99–105.
[35] X.M. He, X.C. Liang, X. Chen, et al., Anal. Chem. 89 (2017) 9712–9721.
[36] X. Zou, J. Jie, B. Yang, Chem. Commun. 52 (2016) 3251–3253.
[37] X. Zou, J. Jie, B. Yang, Anal. Chem. 89 (2017) 7520–7526.
[38] J. Jie, D. Liu, X. Zou, Chem. Commun. 56 (2020) 908–911.
[39] Z. Wang, R. Wu, H. Chen, et al., Nanoscale 10 (2018) 5335–5341.
[40] B. Jiang, Y. Liang, Q. Wu, et al., Nanoscale 6 (2014) 5616–5619.
[41] A. Shen, Z. Guo, L. Yu, et al., Chem. Commun. 47 (2011) 4550–4552.
[42] Y. Zhang, H. Jing, B. Meng, et al., J. Chromatogr. A 1610 (2020) 160545.
[43] Y. Wu, H. Lin, Z. Xu, et al., Anal. Chim. Acta 1096 (2020) 1–8.
[44] W. Ma, L. Xu, X. Li, et al., ACS Appl. Mater. Interfaces 9 (2017) 19562–19568.
[45] Z. Zhou, S. Lin, T. Yue, T. Lee, J. Food Eng. 126 (2014) 133–141.
[46] Z. Xu, J. Zhang, L. Cong, et al., J. Sep. Sci. 34 (2011) 46–52.
[47] D. Jiang, Z. Li, Q. Jia, Anal. Chim. Acta 1066 (2019) 58–68.
[48] H. Zheng, L. Jiang, Q. Jia, Chem. J. Chin. Univ. 42 (2021) 717–724.
[49] S.P. Kuang, Z.Z. Wang, J. Liu, Z.C. Wu, J. Hazard. Mater. 260 (2013) 210–219.